J Therm Anal Calorim (2016) 126:1015–1021
DOI 10.1007/s10973-016-5816-9

Calorimetric study of Eu_2O_3–ZrO_2 feedstock powders and sintered materials

Sebastian Jucha[1] · Grzegorz Moskal[2] · Marta Mikuśkiewicz[2] · Michał Stopyra[2]

Received: 16 November 2015 / Accepted: 4 September 2016 / Published online: 14 September 2016

Abstract The synthesis of ceramic materials based on europia–zirconia system and obtained by solid-state reaction in high-temperature vacuum press was investigated. Firstly, phase composition and calorimetric behavior of feedstock powders was investigated. The second part of the paper concerns the synthesis process of non-stoichiometric mixtures of feedstock powders prepared by four different methods of mixing. The influence of the homogenization method on the calorimetric behavior and phase composition of obtained sinters was studied. Finally, the influence of the additional high-temperature annealing was also investigated. From the obtained results, it can be concluded that the mixing procedure had a very strong influence on the morphology of obtained sinters. This is due to the structural inhomogeneity, as indicated by differences in phase composition. The synthesis process has a gradual character, and the obtaining of materials with different level of homogeneity allowed the determination of the order of subsequent intermediate phase formation.

✉ Grzegorz Moskal
grzegorz.moskal@polsl.pl

Sebastian Jucha
sebastian.jucha@polsl.pl

Marta Mikuśkiewicz
marta.mikuskiewicz@polsl.pl

Michał Stopyra
michal.stopyra@polsl.pl

[1] Department of Production Engineering, Silesian University of Technology, ul. Krasińskiego 8, 40-019 Katowice, Poland

[2] Institute of Materials Science, Silesian University of Technology, ul. Krasińskiego 8, 40-019 Katowice, Poland

Keywords Europium zirconates · Solid state synthesis · DSC analysis

Introduction

Ceramics from ZrO_2–RE_2O_3 system attracts scientific attention, particularly in terms of synthesis and sintering of nano-powders [1, 2]. Rare earth zirconates are promising group of ceramic materials with very high application potential including, e.g., ceramic insulation layers in thermal barrier coatings (TBC) systems. Ceramic materials for insulating layer of TBC have to meet several requirements: minimum thermal conductivity, thermal stability at high temperature, thermochemical compatibility with alumina and good fracture toughness [3–5].

Some of rare earth zirconates exhibit a so-called pyrochlore type of crystal structure. Pyrochlore unit cell can be perceived as eight elementary cells of fluorite, each of which comprises on average a single oxygen vacancy. The stoichiometric general formula of pyrochlore structure is $A_2^{3+}B_2^{4+}O_7$, where A-cations are usually rare earth metals, and B-cations are transition metals [5–8]. The most promising materials from this group as potential candidates for topcoat in TBC systems proved to be La, Gd, Nd, Sm and Eu zirconates. These compounds exhibit many desirable properties, a very low coefficient of thermal conductivity, below 2.0 W m^{-1} K^{-1}; a high coefficient of thermal expansion $>10^{-5}$ $°C^{-1}$; a working temperature up to 1600 °C [9–13].

Recently, some interesting data concerning non-stoichiometric zirconates with fluorite/pyrochlore type of lattice were reported, e.g., better insulating properties [14]. The synthesis of non-stoichiometric europium zirconate and investigation of this process from a calorimetric point of view is the aim of this article.

Research methodology

The differential scanning calorimetry (DSC) experiments were performed on DSC 404 F1 Netzsch apparatus in the single cycle of heating and cooling from room temperature to 1450 °C. Heating and cooling rate was 5 °C min^{-1}, and alumina crucibles were used. Both feedstock oxides (Eu_2O_3, ZrO_2) and their mixtures were studied. The mixtures were prepared via four different methods:

- dry mechanical mixing (DM);
- mechanical milling in alcohol (MA);
- ultrasound-assisted mixing in alcohol (USA);
- mechanical milling in alcohol with additional ultrasound-assisted mixing in alcohol (MUA).

The investigation was also carried out for the sinters obtained via high-temperature sintering under pressure (HTSP). HTSP process was realized in high-temperature vacuum press. The sintering parameters were 1350 °C/15 MPa/2 h with heating and cooling rate 15 °C min^{-1}. Phase analysis was performed using X-ray diffraction (Jeol JDX-7S), both on starting oxides and sinters. Investigated mixtures contained Eu_2O_3 and ZrO_2 in 1:1 mass ratio.

Results

Results of this analysis for zirconia powder (Fig. 1a) revealed the presence of only one phase—monoclinic ZrO_2. The results of phase analysis of Eu_2O_3 powder (Fig. 1b) indicate the presence of two phases: cubic Eu_2O_3 (C) and monoclinic Eu_2O_3 (M), as indicated by the small peaks, which cannot be attributed to Eu_2O_3 (C).

The calorimetric curves for feedstock powders are presented in Fig. 2. DSC investigation of Eu_2O_3 powder revealed the presence of three different endothermic reactions during heating (Fig. 2a) with no reverse reactions during cooling (Fig. 2b). The first peak (285 °C) may be attributed to the dehydration effect. In [15], similar effects were reported for Nd_2O_3 and La_2O_3. Similar endothermal peaks at 225 and 295 °C were attributed to decomposition of $Nd(OH)_3$ and $La(OH)_3$, respectively. The peaks at 968 and at 1178 °C have much lower intensity (−4.13 and −1.88 J g^{-1}, respectively), which makes them more difficult for clear interpretation. Regardless of the reactions type, strong effect of heat flow decreasing was observed at temperature higher than approx. 1100 °C. In DSC curves obtained from ZrO_2 feedstock powder, two strong thermal effects could be observed: endothermic reaction during heating (−25.52 J g^{-1}), which is attributed to a phase transformation from monoclinic to tetragonal zirconia (1186 °C) and reverse transformation during cooling at temperature 1028 °C (30.59 J g^{-1}). Additionally, at high temperature (above ∼1100 °C) strong decrease in heat flow was observed, as in the case of Eu_2O_3.

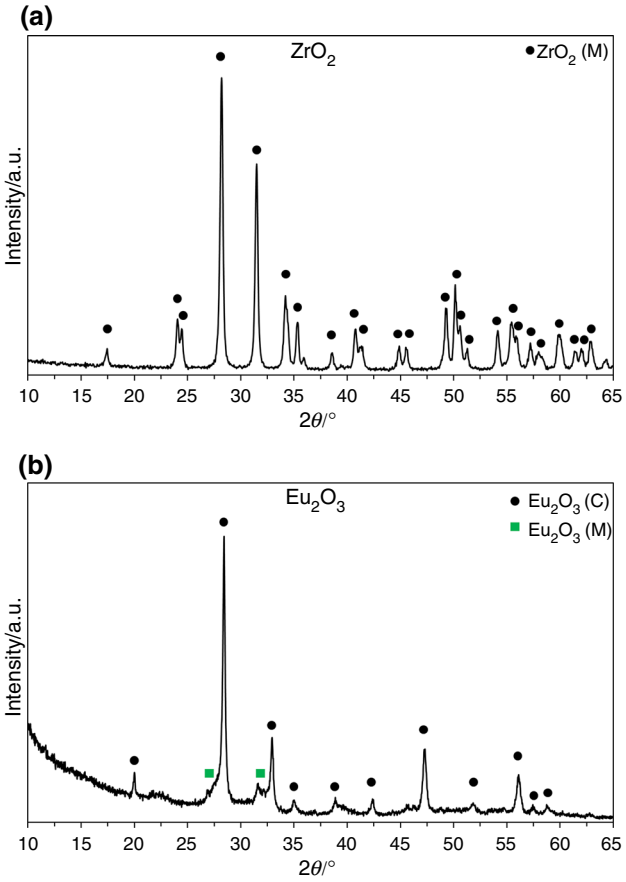

Fig. 1 Diffraction patterns form ZrO_2 (**a**) and Eu_2O_3 (**b**) feedstock powders

DSC investigation of mixed feedstock oxides included the calorimetric analysis of prepared powders in as-mixed condition and after consolidation via high-temperature sintering process under pressure. Calorimetric curves for mixed powders prepared using different method of homogenization are presented in Fig. 3. No clear evidence for the synthesis of new compound can be seen; however, comparison of the curves for input powders and their mixture leads to following conclusions:

(a) the apparent lack of a reverse peaks from tetragonal to monoclinic phase transformation of zirconia during cooling of mixtures homogenized using MA, USA, MUA methods, in the case of DM mixture the intensity if this peak is strongly reduced (2.64 J g^{-1});
(b) similarly to the feedstock powders, decline in heat flux was observed in all mixtures at high temperature.

All calorimetric curves have similar shape in the heating range. The effects of dehydration of Eu_2O_3 are observed at temperature 272 °C for DM, 273 °C for USA and in

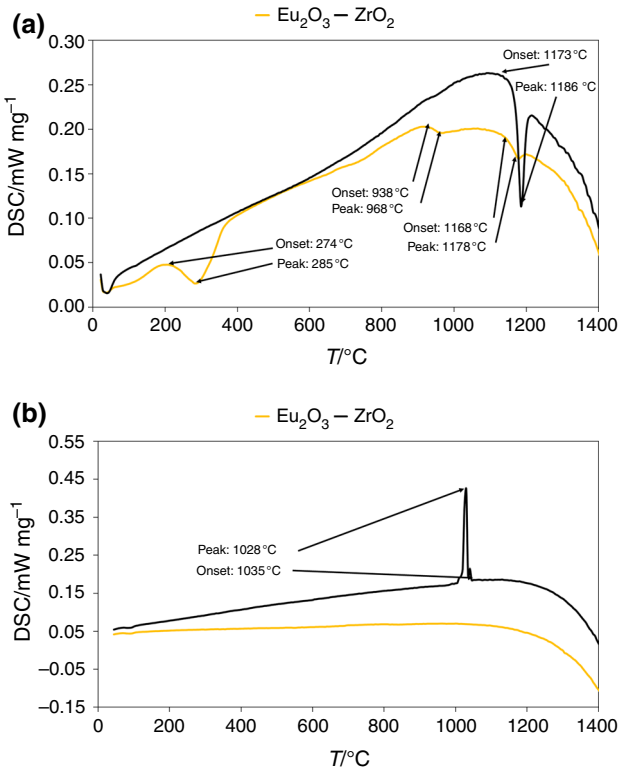

Fig. 2 DSC curves form Eu_2O_3 and ZrO_2 feedstock powders: heating (**a**) and cooling (**b**)

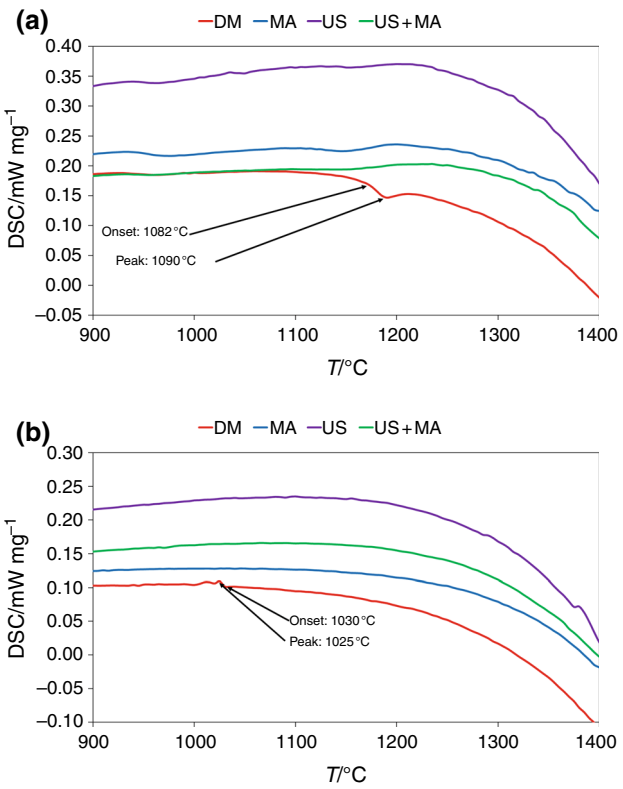

Fig. 3 DSC curves form ZrO_2 and Eu_2O_3 powders mixed via DM, AM, US and USA methods: heating (**a**) and cooling (**b**)

269 °C for MUA mixtures. Phase transformation of Eu_2O_3 (C → B) and ZrO_2 (M → T) occurs at similar temperature which makes the interpretation of peaks in the range 1150–1190 °C more difficult.

The shapes of DSC curves obtained from as-sintered samples (Fig. 4) are of completely different character than in the case of starting powders and their mixtures. Firstly, the strong heat flux decrease during heating at high temperature was no longer present in the sinters. It indicates that in the case of powders the decrease of DSC signal is caused by sintering. In general, sintering is an exothermal process because the surface energy of powder is higher than the energy of grain boundaries. However, reduction of material's porosity during the DSC investigation changes the conditions of heat transfer through the sample and the holder, which in turn influences the measured signal. The shrinkage of the material reduces the contact area between the sample and the surface of the holder and hinders the energy transfer. In the case of the curves obtained from sintered materials, this phenomenon is not observed, because the temperature during the investigation is too low to cause any further densification of samples. Similar effects were observed in [16].

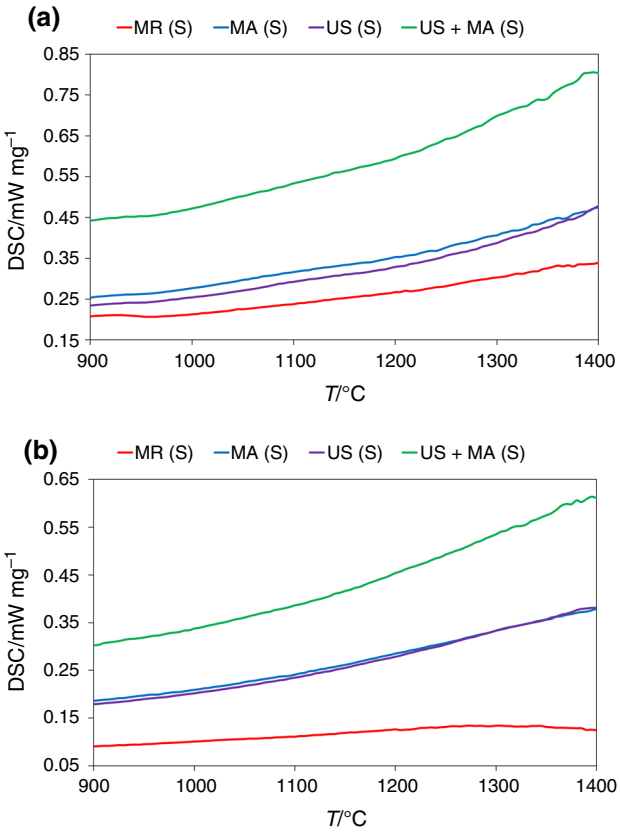

Fig. 4 DSC curves form ZrO_2–Eu_2O_3 sinters obtained from powders mixed via DM, AM, US and USA methods: heating (**a**) and cooling (**b**)

Thermal effects indicating phase transformations were present only in the case of the sinter obtained from DM mixture: an endothermic peak (-11.85 J g^{-1}) at 961 °C (during heating) and the exothermic peak (31.93 J g^{-1}) at 1273 °C (during cooling). Those peaks are due to phase transformations of residual ZrO_2 which remained unreacted due to the inhomogeneity of mixture or to the phase transformation of non-stoichiometric compounds from Eu_2O_3–ZrO_2 system. In the sinters obtained from AM, USA and MUA mixtures, those types of effect were not observed in this scale of intensity.

The results of phase analysis of sinters are presented in Fig. 5. Generally, in all investigated variants of powders mixing method, the new phases were detected, which is due to the high-temperature solid-state reaction. The predominant phase was identified as europium zirconate $Eu_2Zr_2O_7$ with defected fluorite (Fm-3m) type of lattice. The most inhomogeneous material in terms of phase composition was the sinter obtained from DM mixture, in which other zirconate phases were detected as well, both non-stoichiometric ($Eu_{0.2}Zr_{0.8}O_{1.9}$) and stoichiometric ($Eu_{0.5}Zr_{0.5}O_{1.75}$). Additionally, in the DM sinter two other phases were present: complex oxide with crystal lattice isomorphic to $(Eu,Lu_{0.5},Ta_{0.5})O_3$ (28-0416) which was identified as $(Eu,Zr)_2O_3$ oxide with cubic structure (C) and monoclinic ZrO_2 which is one of the starting materials.

Those oxides and non-stoichiometric zirconates were also present in the sinters obtained from powders homogenized via USA and MUA methods. However, the peaks attributed to the intermediate phases were of relatively small intensity when compared to DM. The most homogenous phase composition was obtained in the case of AM mixed powders—$Eu_2Zr_2O_7$ with defected fluorite type of lattice was the only phase detected using XRD. An additional heat treatment caused further evolution of phase composition of investigated sinters. The structural changes during the annealing are due to the diffusion-driven process of transformation of intermediate, non-stoichiometric phases (e.g., $Eu_{0.2}Zr_{0.8}O_{1.9}$) to stoichiometric $Eu_{0.5}Zr_{0.5}O_{1.75}$. From these results, it can be concluded that the method of preparation of powders mixture had very strong influence on final phase composition of sinters. This influence may be expressed through the type and number of detected phases which indicate greater or lesser structural homogeneity of sintered materials.

The analysis of XRD patterns allows describing the process of formation final phase, determined by the ratio of constituent oxides in the mixture, in this case—non-stoichiometric europium zirconate. Obtaining of sinters with different structural homogeneity allowed revealing the order of intermediate phase formation during the synthesis process. At first, the mutual dissolution of starting oxides took place, which lead to the formation of binary oxide

Fig. 5 XRD patterns of ZrO_2–Eu_2O_3 sinters obtained from powders before and after heat treatment (+HT) mixed by **a**, **b** DM, **c**, **d** AM, **e**, **f** USA and **g**, **h** MUA methods before and after additional heat treatment at temperature 1450 °C/5 h

$(Eu,Zr)_2O_3$ with cubic structure. On the other hand, as a result of dissolution of europia in ZrO_2 another oxide—$(Zr,Eu)O_2$—with tetragonal or cubic lattice could be formed. This reaction can be described as follows:

$$Eu_2O_3(C) + ZrO_2(M) \rightarrow (Eu,Zr)_2O_3(C) + (Zr,Eu)O_2(T/C) \quad (1)$$

In the next step, non-stoichiometric europium zirconates with fluorite type of lattice were formed, e.g., $Eu_{0.2}Zr_{0.8}O_{1.9}$ which was the result of mutual dissolution of complex oxides mentioned earlier.

$$(Eu,Zr)_2O_3 + (Zr,Eu)O_2 + Eu_2O_3(C) + ZrO_2(M) \rightarrow Eu_{0.2}Zr_{0.8}O_{1.9}(F) + Eu_{0.5}Zr_{0.5}O_{1.75}(F) + Eu_2Zr_2O_7(P) \quad (2)$$

Due to the strong inhomogeneity of mixed powders, these reactions may proceed at the same time, depending on the local concentration of ZrO_2 and Eu_2O_3, wherein the formation of the non-stoichiometric phases with increased content of Zr is promoted by the excessive content of this ZrO_2 in the starting powders mixture.

The non-stoichiometry of the compound is conducive to structural disorder, because both A^{3+} and B^{4+} cations occupy specific crystallographic positions in $A_2B_2O_7$ pyrochlore-type lattice. This is why the formation of superstructure, which results from ordering both in cationic and anionic sublattices, is prone to the disturbance of ratio of A and B contents. In perfect, stoichiometric europium zirconate this ratio should be equal to 1. However, as the excessive content of ZrO_2 is introduced, the system is driven toward defected fluorite. Hence, the small peaks attributed to superstructure are present in the sinters with high structural inhomogeneity—DM, USA and MUA, whereas in the case of the most homogeneous one—AM—the excessive Zr^{4+} cations are most evenly distributed and as a consequence they can be built in $Eu_2Zr_2O_7$ solid solution instead of forming intermediate non-stoichiometric phases.

After additional heat treatment, the structural inhomogeneity was reduced and the subsequent phases with higher level of stoichiometry were formed. An exemplary process could be described in the following way:

$$Eu_{0.2}Zr_{0.8}O_{1.9} \rightarrow Eu_{0.5}Zr_{0.5}O_{1.75} \rightarrow Eu_2Zr_2O_7 \quad (3)$$

The comparison of XRD patterns obtained for as-sintered and heat-treated DM sinter (Fig. 6) gives a clearer idea of the evolution of phase composition during solid-state synthesis of $Eu_2Zr_2O_7$. It can be seen that intensity of

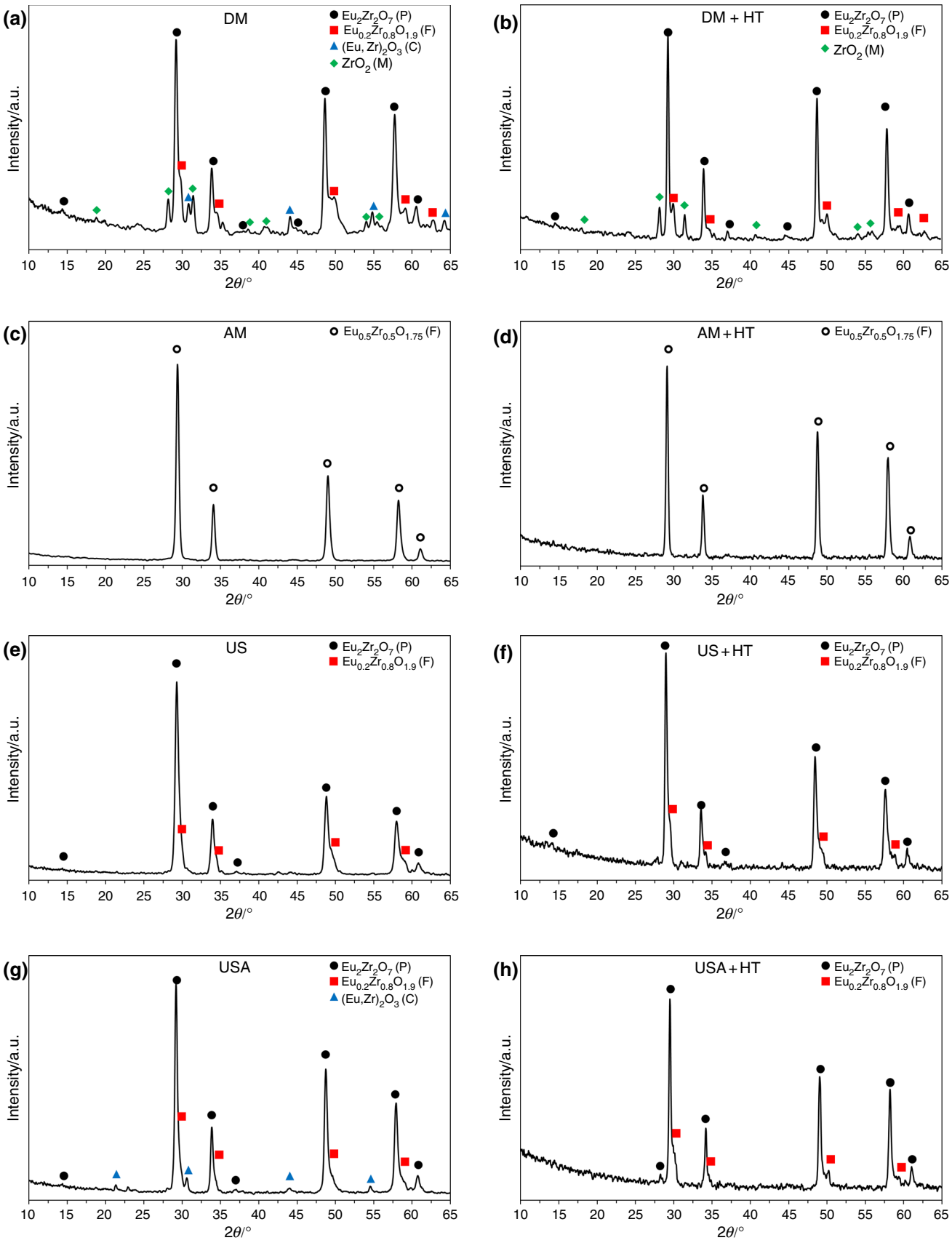
(a)
DM
$Eu_2Zr_2O_7$ (P)
$Eu_{0.2}Zr_{0.8}O_{1.9}$ (F)
$(Eu, Zr)_2O_3$ (C)
ZrO_2 (M)
(b)
DM + HT
$Eu_2Zr_2O_7$ (P)
$Eu_{0.2}Zr_{0.8}O_{1.9}$ (F)
ZrO_2 (M)
(c)
AM
$Eu_{0.5}Zr_{0.5}O_{1.75}$ (F)
(d)
AM + HT
$Eu_{0.5}Zr_{0.5}O_{1.75}$ (F)
(e)
US
$Eu_2Zr_2O_7$ (P)
$Eu_{0.2}Zr_{0.8}O_{1.9}$ (F)
(f)
US + HT
$Eu_2Zr_2O_7$ (P)
$Eu_{0.2}Zr_{0.8}O_{1.9}$ (F)
(g)
USA
$Eu_2Zr_2O_7$ (P)
$Eu_{0.2}Zr_{0.8}O_{1.9}$ (F)
$(Eu,Zr)_2O_3$ (C)
(h)
USA + HT
$Eu_2Zr_2O_7$ (P)
$Eu_{0.2}Zr_{0.8}O_{1.9}$ (F)
Intensity/a.u.
2θ/°
10 15 20 25 30 35 40 45 50 55 60 65

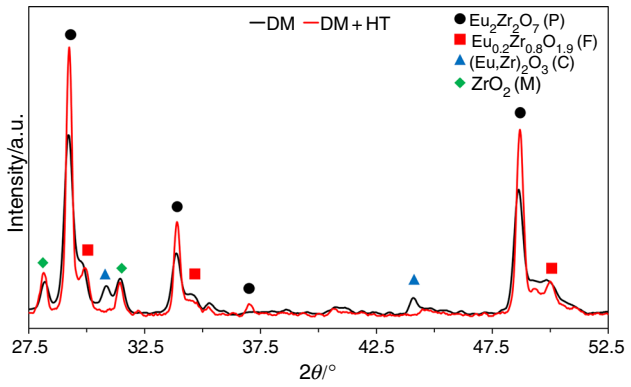

Fig. 6 Close-up of XRD patterns of ZrO_2–Eu_2O_3 sinters obtained from powders mixed by DM method before and after additional heat treatment at 1450 °C/5 h

peaks attributed to the intermediate phases is reduced at the expense of increased intensity of $Eu_2Zr_2O_7$ peaks. The cubic $(Eu,Zr)_2O_3$ phase completely disappeared after annealing. Another difference is the presence of 331 superlattice peak at $2\Theta = 37.2°$ ($d = 2.41$ Å). The ordering of crystal structure, namely the transition from defected fluorite to ordered pyrochlore, is thermally activated, and the temperature of this transition depends on the ratio of ionic radii of A^{3+} and B^{4+} cations. It was reported in [17] that the temperature of F–P transition for $Eu_2Zr_2O_7$ is ca. 1200 °C. However, even in stoichiometric Eu zirconate sintered at 1300 °C, the relative intensity of superstructure peaks was relatively low [18], while in [19] fully ordered europium zirconate was obtained after synthesis at 1400 °C. In the present study, the temperature of additional heat treatment was 1450 °C which is enough to form ordered pyrochlore from defected fluorite. In the case of AM sample with single phase composition, this transformation did not occur, because the excessive ZrO_2 disturbed Eu/Zr ratio prevented the ordering of crystal structure. In the case of DM sample with single phase composition, excessive ZrO_2 was concentrated in intermediate phases, allowing the formation of ordered pyrochlore-type $Eu_2Zr_2O_7$ from defected fluorite-type $Eu_{0.5}Zr_{0.5}O_{1.75}$ at high temperature.

Conclusions

Calorimetric studies of ZrO_2–Eu_2O_3 feedstock powders mixed by four various methods (DM, MA, USA and MUA), showed that the mixture preparation process has a strong influence on the character of DSC curves. This is the effect of strong inhomogeneity of powders mixture obtained in the DM process and relatively high homogeneity obtained in MA, USA and MUA processes. From the results, it can be concluded that MA process is the most suitable one in terms of homogenization.

Strong endothermal effect observed during primary heat treatment (synthesis) above the temperature ca. 1200 °C is related probably to so-called parasitic heat capacity. XRD phase analysis revealed that new zirconate phases of $Eu_{0.2}Zr_{0.8}O_{1.9}$, $Eu_{0.5}Zr_{0.5}O_{1.75}$ and $Eu_2Zr_2O_7$ types were formed.

This interpretation of observed phenomena could be confirmed by DSC investigation of final sinters made by HTSP method. In this case a drop of heat flux signal was not observed, instead the signal continuously increased with increase in temperature. Similar results were obtained for sinters made by HTSPA method.

The only effect observed during DSC analysis of sinters before and after additional annealing was related to homogenization of chemical composition of sinters at 1450 °C. Those effects were also confirmed by XRD analysis of phases constituent, and they are typical for solid-state sintering processes.

Acknowledgements Financial support of Structural Funds in the Operational Program—Innovative Economy (IE OP) financed from the European Regional Development Fund—Project No POIG.0101.02-00-015/09 is gratefully acknowledged.

References

1. Batista RM, Muccillo ENS. Dilatometry analysis of the sintering process of nanostructured gadolinia-doped ceria. J Therm Anal Calorim. 2016. doi:10.1007/s10973-016-5674-5.
2. Surzhikov AP, et al. A thermoanalysis of phase transformations and linear shrinkage kinetics of ceramics made from ultrafine plasmochemical $ZrO_2(Y)$–Al_2O_3 powders. J Therm Anal Calorim. 2014;115:1439–45.
3. Toritz FC, et al. Thermal barrier coatings for jet engines. ASME-88-GT-279. 1;1988.
4. Sheffler KD, Gupta DK. Current status and future trends in turbine application of thermal barrier coatings. ASME-88-GT-286. 1;1988.
5. Meier SM, et al. Thermal barrier coating life prediction model. Trans ASME. 1992;114:258.
6. Malony MJ. U.S. Patent 6, 284,323;2001.
7. Subramanian R. U.S. Patent 6,387,539;2002.
8. Vassen R, et al. New thermal barrier coatings based on pyrochlore/YSZ double-layer systems. Int J Appl Ceram Technol. 2004;1:351–61.
9. Moskal G, et al. Characterization of thermal properties of micro-sized ceramic powders for APS deposition of ceramic layers. Key Eng Mater. 2011;484:152–7.

10. Moskal G. Microstructure and thermal diffusivity of RE zirconate powders for TBC system obtained by the APS method. In: Gaal DS, Gaal PS, editors. Proceedings of the 30th international thermal conductivity conference and 18th international thermal expansion symposium. Pittsburgh: DEStech Publications, Inc.; 2009. p. 451–6.
11. Moskal G, Dercz G. Effect of heat treatment on structure and phase transformation of rare earth (Gd) zirconate. Solid State Phenom. 2010;163:157–60.
12. Moskal G, et al. Characteristics of phenomena in powders type $RE_2Zr_2O_7$–Al_2O_3 in high temperature annealing conditions. Defect Diff Forum. 2011;312–315:583–8.
13. Moskal G, et al. Characteristics of thermal properties of $Gd_2Zr_2O_7$–$ZrO_2 \times Y_2O_3$ powder mixtures intended for deposition of gradient layers of TBC type. Defect Diff Forum. 2011;312–315:577–82.
14. Shlyakhtina AV, et al. Effect of non-stoichiometry and synthesis temperature on the structure and conductivity of $Ln_2 + xM_2 - xO_{7-x/2}$ (Ln = Sm–Gd; M = Zr, Hf; x = 0–0.286). Solid State Ion. 2007;178:59–66.
15. Fedorov PP, et al. On polymorphism and morphotropism of rare earth sesquioxides. Crystallogr Rep. 2002;47:316–21.
16. Souza JP, Martinelli JR. Evaluation of aluminosilicate glass sintering during differential scanning calorimetry. Ceram Int. 2015;41:7296–301.
17. Michel D, et al. Study by Raman spectroscopy of order-disorder phenomena occurring in some binary oxides with fluorite-related structures. J Raman Spectrosc. 1976;5:163–80.
18. Stopyra M, et al. Synthesis and thermal properties of europium zirconate and hafnate via solid state reaction and polymerized complex method. Surf Coat Technol. 2015;284:38–43.
19. Maram PS, et al. In situ diffraction from levitated solids under extreme conditions—structure and thermal expansion in the Eu_2O_3–ZrO_2 system. J Am Ceram Soc. 2015;98:1292–9.